Interaction of the Important Species HNO and $HFSO_2$ in the Atmosphere: Theoretical Study of the N—H and S—H Blue-Shifted Hydrogen Bonds

YING LIU,[1,3] WENQING LIU,[1] HAIYANG LI,[2] YONG YANG,[1,3] SHUANG CHENG[1,3]

[1]*Key Laboratory of Environmental Optical and Technology, Anhui Institute of Optics and Fine Mechanics, Chinese Academy of Sciences, Hefei 230031, People's Republic of China*

[2]*Dalian Institute of Chemical Physics, Chinese Academy of Sciences, Dalian 116023, People's Republic of China*

[3]*Graduate School of Chinese Academy of Sciences, Beijing 100039, People's Republic of China*

Received 14 February 2006; accepted 30 March 2006
Published online 22 September 2006 in Wiley InterScience (www.interscience.wiley.com).
DOI 10.1002/qua.21077

ABSTRACT: Ab initio molecular orbital and density functional theory (DFT) in conjunction with different basis sets calculations were performed to study the N—H···O and S—H···O blue-shifted H-bonds in the HNO···$HFSO_2$ complex. The geometric structures, vibrational frequencies, and interaction energies were calculated by both standard and CP-corrected methods. Natural bond orbital (NBO) analysis was used to investigate the origin of blue-shifted H-bonds, showing that the decrease in the σ^*(N—H) and σ^*(S—H) is due to the electron density redistribution effect. The structure reorganization effect on the blue-shifted hydrogen bonds was discussed in detail.

Key words: blue-shifted hydrogen bond; electron density redistribution; structure reorganization; rehybridizative effect

Introduction

Hydrogen bonding is an important type of noncovalent interaction that is present in many chemical and biological systems [1]. A sound knowledge of H-bonding is fundamental to understanding chemical structures, enzyme catalysis, material properties, self-assembly phenomena, and functions of molecular and biological devices and machines. Therefore, considerable experimental and theoretical research has been conducted concerning the structural, spectroscopic, and energetic issues of diverse H-bonds [2–4]. Most hydrogen bonds are of X—H···Y type, where X is an electronegative atom and Y is either an electronegative atom having one or more lone electron pairs, or a

Correspondence to: Y. Liu; e-mail: lying@aiofm.ac.cn
Contract grant sponsor: Center for Computational Science, Hefei Institutes of Physical Sciences.
Contract grant number: 0330405002.

region excess electron density such as aromatic π-system [5]. Recently, a new type of intermolecular bonding, termed blue-shifting hydrogen bond, accompanied by X—H bond contraction and a blue shift of the X—H bond stretching frequency, continues to receive significant experimental and theoretical attention [6–15]. The blue-shifting H-bonds studied so far are mainly C—H···Y systems, such as C—H···N, C—H···O and C—H···F [8, 11, 16]. To rationalize the C—H bond shortening and the consequent blue shift of the C—H stretching frequency, two explanations have been proposed [17]. Recently, Yang et al. [18] confirmed the N—H···O H-bond blue shifts by theoretical calculations. However, to the best of our knowledge, the researches on S—H···O blue-shifted hydrogen bond systems are scarce.

Species containing N (e.g., HNO and HNO_2) and containing S (e.g., H_2SO_2 and $HFSO_2$) are important in the atmosphere chemistry and combustion chemistry, hence many theoretical and experimental studies were performed [19–21]. The C—H and N—H blue-shifted hydrogen bonds involving HNO have been reported by our group [18]. The HNO···$HFSO_2$ system is involved in the N—H···O and S—H···O blue-shifted H-bonds. It is helpful to give more information about the N—H···O and give S—H···O blue-shifted hydrogen bonds that the investigations were performed on HNO···$HFSO_2$ system.

In the present work, we perform ab initio molecular orbital and density functional theory (DFT) in conjunction with different basis sets calculations [both standard and counterpoise (CP) calculations] to report the optimized structures, interaction energies, and vibrational frequencies of the HNO···$HFSO_2$ complex. The S—H···O blue-shifted H-bond is confirmed for the first time. In addition, we confirm the existence of the N—H···O blue shift H-bond. Natural bond orbital (NBO) analysis and partial optimization were carried out to provide reasonable explanations of the origin of N—H and S—H blue shifts by hyperconjugation, rehybridization, electron density redistribution, and structure reorganization. Our aim is to predict the existence of N—H···O and S—H···O blue-shifted H-bonds and to give more insight into the nature of the blue shifts.

Computational Details

The HNO···$HFSO_2$ complex was investigated by different theoretical methods, including DFT (Becke's three-parameter hybrid functional in conjunction with Lee, Yang, and Parr's correlation functional, abbreviated B3LYP) and second-order Møller–Plesset perturbation (MP2) methods [Hartree–Fock (HF) calculation, followed by Møller–Plesset correlation energy correction truncated at second order] in conjunction with different basis sets. Both standard and CP-corrected gradient optimization was performed, followed by vibrational frequency calculations, to confirm the actual minima obtained. Basis set superposition errors (BSSE) were calculated according to the CP method proposed by Boys and Bernardi [22]. In addition, interaction energies were calculated at the G2MP2 levels. NBO analysis was performed at the B3LYP/6-311+G** level [23]. Partial optimization was carried out at both the B3LYP/6-311+G** and MP2/6-311+G** levels. All calculations were carried out using the Gaussian-03 package [24].

Results and Discussion

GEOMETRIES, FREQUENCIES, AND INTERACTION ENERGIES

The characteristics of the HNO···$HFSO_2$ complex, determined by both standard and CP-corrected optimization and stretching frequency changes between the complex and monomers, are presented in Table I and Figure 1. The structure and vibrational frequencies are calculated using the MP2 and B3LYP methods with the 6-31G*, 6-311+G**, and 6-311++G(2*d*,2*p*) basis sets. O-site ($HFSO_2$) H-bond forming in the complex is considered the minimum. However, one imaginary vibrational frequency of the F site ($HFSO_2$) H-bond formation in the complex appears by calculation and is not discussed further in the present work.

Recently, Hobza and Havlas [25] pointed out the necessity of CP-corrected gradient optimization for H-bond blue-shift research. We performed the CP-corrected calculations for structure optimizations, vibrational frequencies, and interaction energies. All corrected H-bond distances, N7—H8 and S1—H4 bond lengths, are a little longer than uncorrected ones, except for the B3LYP/6-311++G(2*d*,2*p*) level.

From the stretching frequency changes between the HNO···$HFSO_2$ complex and the monomers shown in Table I, as far as the H-bond type prediction is concerned, the MP2 computation results are in agreement with those of B3LYP. All indicate that both the N7—H8 and S1—H4 stretching frequen-

TABLE I

Characteristics of HNO, $HFSO_2$, and HNO· · ·$HFSO_2$ complex at B3LYP, MP2 level in conjunction with different basis sets and interaction energies obtained at G2MP2 level.*

	6-31G*	6-311+G**	6-311++G(2*d*,2*p*)
		B3LYP	
$r^{standard}$ (O2· · ·H8)(Å)	2.1793	2.2169	2.2678
r^{CP} (O2 . . . H8) (Å)	2.2334	2.2653	2.3036
$r^{standard}$ (O6 . . . H4) (Å)	2.5327	2.533	2.5901
r^{CP} (O6 · · ·H4) (Å)	2.6134	2.5491	2.5851
$\Delta r^{standard}$ (N7· · ·H8) (Å)	−0.0087	−0.0049	−0.0044
Δr^{CP} (N7—H8) (Å)	−0.0069	−0.0048	−0.0046
$\Delta r^{standard}$ (S1—H4) (Å)	−0.0062	−0.0042	−0.004
Δr^{CP} (S1—H4) (Å)	−0.0053	−0.0037	−0.0037
$\Delta\nu^{standard}$ (N7—H8) (cm^{-1})	+141	+98	+92
$\Delta\nu^{CP}$ (N7—H8) (cm^{-1})	+115	+95	+92
$\Delta\nu^{standard}$ (S1—H4) (cm^{-1})	+51	+34	+36
$\Delta\nu^{CP}$ (S1—H4) (cm^{-1})	+45	+31	+32
$\Delta E^{standard}$ (kcal/mol)	−4.48	−3.57	−2.70
ΔE^{CP} (kcal/mol)	−2.33	−2.82	−2.27
		MP2	
$r^{standard}$ (O2· · ·H8) (Å)	2.2204	2.2476	2.2459
r^{CP} (O2· · ·H8) (Å)	2.335	2.3532	2.3388
$r^{standard}$ (O6· · ·H4) (Å)	2.6024	2.6074	2.6065
r^{CP} (O6· · ·H4) (Å)	2.6844	2.68	2.6492
$\Delta r^{standard}$ (N7—H8) (Å)	−0.0061	−0.0034	−0.0025
Δr^{CP} (N7—H8) (Å)	−0.005	−0.0032	−0.0027
$\Delta r^{standard}$ (S1—H4) (Å)	−0.0045	−0.0041	−0.0031
Δr^{CP} (S1—H4) (Å)	−0.0038	−0.0031	−0.0028
$\Delta\nu^{standard}$ (N7—H8) (cm^{-1})	+115	+80	+69
$\Delta\nu^{CP}$ (N7—H8) (cm^{-1})	+94	+74	+67
$\Delta\nu^{standard}$ (S1—H4) (cm^{-1})	+41	+36	+33
$\Delta\nu^{CP}$ (S1—H4) (cm^{-1})	+38	+30	+30
$\Delta E^{standard}$ (kcal/mol)	−5.23	−4.46	−4.16
ΔE^{CP} (kcal/mol)	−2.62	−2.61	−2.90
ΔE_{G2MP2} (kcal/mol)			−3.99

* Standard: values obtained without counterpoise correction from the energy and from the geometry optimization; CP: the values obtained both by counterpoise correction from the energy and from the geometry optimization.

cies have blue shifts in the complex. The CP-corrected gradient optimization will affect not only the interaction energy but also the geometry and stretching frequency of the X—H· · ·Y H-bond. However, the blue shifts of the N7—H8 and S1—H4 stretching frequencies in the complex by B3LYP and MP2 calculations still exist, as shown in Table I, in spite of application of the CP-corrected calculations. In contrast, the blue shifts of the N7—H8 and S1—H4 stretching frequencies by CP-corrected optimizations are slightly smaller but are still in reasonable agreement with those of the N7—H8 and S1—H4 stretching frequencies by stan-

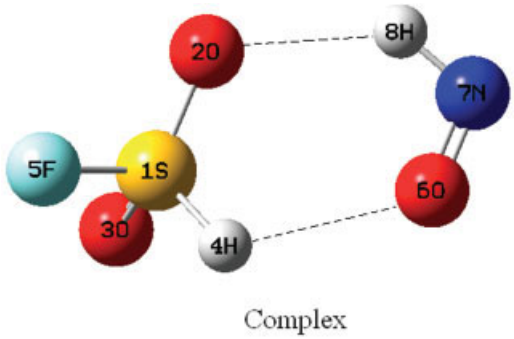

FIGURE 1. Optimized structure of HNO· · ·$HFSO_2$ complex. [Color figure can be viewed in the online issue, which is available at www.interscience.wiley.com.]

TABLE II

NBO analysis of the HNO, $HFSO_2$ monomers and HNO···$HFSO_2$ complex at the B3LYP/6-311+G level.**

	HNO	$HFSO_2$	HNO···$HFSO_2$ complex
$E^{(2)}$ σ(S1—O2) → σ^*(S1—H4) (kcal mol^{-1})	—	1.93	1.68
$E^{(2)}$ σ(S1—O3) → σ^*(S1—H4) (kcal mol^{-1})	—	1.93	1.69
$E^{(2)}$ σ(S1—H4) → σ^*(S1—H4) (kcal mol^{-1})	—	1.69	1.46
$E^{(2)}$ σ(S1—F5) → σ^*(S1—H4) (kcal mol^{-1})		2.42	2.40
$E^{(2)}$ $_{CR}$(S1) → σ^*(S1—H4) (kcal mol^{-1})		0.66	0.57
$E^{(2)}$ n_1(O2) → σ^*(S1—H4) (kcal mol^{-1})		16.38	15.12
$E^{(2)}$ n_2(O2) → σ^*(S1—H4) (kcal mol^{-1})	—	4.55	3.87
$E^{(2)}$ n_3(O2) → σ^*(S1—H4) (kcal mol^{-1})			0.56
$E^{(2)}$ n_1(O3) → σ^*(S1—H4) (kcal mol^{-1})		16.38	15.58
$E^{(2)}$ n_2(O3) → σ^*(S1—H4) (kcal mol^{-1})		4.55	4.35
$E^{(2)}$ n_3(O3) → σ^*(S1—H4) (kcal mol^{-1})			0.58
$E^{(2)}$ n_1(*F*5) → σ^*(S1—H4) (kcal mol^{-1})		3.64	3.56
$E^{(2)}$ n_1(O6) → σ^*(S1—H4) (kcal mol^{-1})			0.21
$E^{(2)}$ n_2(O6) → σ^*(S1—H4) (kcal mol^{-1})			0.11
$E^{(2)}$ n_1(O6) → σ^*(N7—H8) (kcal mol^{-1})	17.52		14.79
$E^{(2)}$ n_1(O2) → σ^*(N7—H8) (kcal mol^{-1})			0.61
$E^{(2)}$ n_2(O2) → σ^*(N7—H8) (kcal mol^{-1})			0.16
$E^{(2)}$ n_3(O2) → σ^*(N7—H8) (kcal mol^{-1})			1.52
$E^{(2)}$ σ^*(S1—O2) → σ^* (N7—H8) (kcal mol^{-1})			0.71
σ^*(N7—H8) (e)	0.05203		0.04717
σ^*(S1—H4) (e)	—	0.19509	0.18504
$R_{E(N7—H8)}$			1.099
$R_{E(S1—H4)}$			0.118
q(H8) (e)	0.24219		0.27902
q(H6) (e)		0.02650	0.05186
% s-char(N7 in N7—H8)	17.83%		19.14%
% s-char(S1 in S1—H4)	—	23.33%	23.77%

dard optimization. On the basis of these analyses, we can confirm that both the N7—H8 and S1—H4 stretching frequencies display blue shifts.

As shown in Table I, the intermolecular interaction energies with both BSSE correction and zero-point vibrational energy (ZPVE) correction are in reasonable agreement at various levels in conjunction with various basis sets. For the weak interactions, the BSSE correction is important for an accurate description of the intermolecular interaction energies. The interaction energies obtained at the MP2/6-311++G(2*d*, 2*p*) level are in good agreement with those obtained at the G2MP2 levels. With the basis sets increasing, the differences between the standard calculations and CP-corrected calculations become smaller.

NBO ANALYSIS

For a better understanding of the origin of the blue-shifted H-bond, NBO analysis has been carried out at the B3LYP/6-311+G** level and the corresponding results are collected in Table II. In general, the hyperconjugative effect increased the electron density in the σ^*(X—H). However, the electron density in the σ^*(X—H) decreased instead of increasing. We pay more attention to an interesting phenomenon, which is the electron density decrease in the σ^*(N7—H8) and σ^*(S1—H4). Hobza and colleagues [6, 26] showed that the decreased electron density in the σ^*(X—H) is caused by the electron density redistribution effect. On the basis of the electron density redistribution effect, we will provide a reasonable model to explain the decreased electron density in the σ^*(X—H) [18]. Owing to the H-bond formation n(Y) interacts with σ^*(X—H), which leads to the change in electron density. In the type (W—) Z—X—H···Y (—U) H-bond, where Z represents electronegative atoms with one or more lone electron pairs (e.g., F, O, N), the hyperconjugative n(Y) or σ(Y—U) → σ^*(X—H) interaction leads to increased electron density in the

σ^*(X—H). In contrast, a decrease in the n(Z) or σ(W—Z) $\rightarrow$ σ^*(X—H) interaction of the complex, relative to the monomer, has the opposite effect. As a result, the net change in the electron density in the σ^*(X—H), and the ultimate direction of the X—H bond length change, depend on the balance of these two interactions, which changed in an antiparallel way. A quantitative comparison between these two interactions was performed as follows:

$$R_E = \frac{\sum E^{(2)}_{\text{increasing}}}{\sum E^{(2)}_{\text{decreasing}}}, \quad (1)$$

where $\sum E^{(2)}_{\text{increasing}} = \sum E^{(2)}[n(\text{Y}) \text{ or } \sigma(\text{Y—U}) \rightarrow \sigma^*(\text{X—H})] + V$, which denotes the n(Y) or σ (Y—U) $\rightarrow$ σ^*(X—H) interaction in the complex. $\sum E^{(2)}_{\text{decreasing}} = \sum(E^{(2)}_{\text{monomer}}[n(\text{Z}) \text{ or } \sigma(\text{Z—W}) \rightarrow \sigma^*(\text{X—H})] - E^{(2)}_{\text{complex}}[n(\text{Z}) \text{ or } \sigma(\text{Z—W}) \rightarrow \sigma^*(\text{X—H})])$. It should be pointed out that if some values of the $E^{(2)}_{\text{monomer}}[n(\text{Z}) \text{ or } \sigma(\text{Z—W}) \rightarrow \sigma^*(\text{X—H})] - E_{\text{complex}}[n(\text{Z}) \text{ or } \sigma(\text{Z—W}) \rightarrow \sigma^*(\text{X—H})]$ are below zero, these should not be included in the $\sum E^{(2)}_{\text{decreasing}}$, and their absolute values should be V. In general, the smaller the value of R_E, the less electron density in the σ^*(X—H) owing to electron density redistribution effect. The larger the value of R_E, the stronger the hyperconjugation and the weaker the electron density redistribution. As shown in Table II, the $R_{E(\text{N7—H8})} = 1.099$ and $R_{E(\text{S1—H4})} = 0.118$; the value of $R_{E(\text{S1—H4})}$ is very small, indicating that the electron density redistribution effect is very significant in the S1—H4$\cdots$O6 H-bond of the complex. The electron density redistribution effect overshadows the hyperconjugative effect, which leads to an evident electron density decrease in the σ^*(S1—H4). For the N7—H8$\cdots$O2 H-bond, the electron density redistribution effect is relatively strong; as a result, it can be seen that the net decrease of electron density in the σ^*(N7—H8) is relatively small. The hyperconjugative effect is overcome by the electron density redistribution effect, which leads to the decreased electron density in σ^*(X—H). This makes the X—H bonds contract and contributes to blue shifts of X—H vibrational frequencies. Recently, Alabugin et al. [27] showed that the change in the X—H bond in the process of both blue-shifted and red-shifted H-bonds was determined by the balance of the opposing effects: the X—H bond lengthening effect due to the hyperconjugative n(Y) $\rightarrow$ σ^*(X—H) interaction and X—H bond shortening effect due to rehybridization. On the basis of the rehybridization model, the N7—H8$\cdots$O2 and S1—H4$\cdots$O6 H-bond formations increase N7—H8 and S1—H4 bond polarization and positive charge on the H8 and H4 atom. As shown in Table II, the s-character of N7 in the complex is a little more than that in the monomer, which contributes to the N7—H8 bond contraction, to some extent. Moreover, the difference for the s-character of S between the complex and monomer is very small.

STRUCTURE REORGANIZATION

NBO analysis gives the origin of the H-bond blue shift in the electron density transfer. The structure change effect of HNO and $HFSO_2$ monomers in the complex on the blue shifts is discussed in this section. To demonstrate the effect of changes of bond lengths, bond angles, dihedral angles on blue shifts of the N—H and S—H vibrational frequencies, the partial optimizations on the HNO and $HFSO_2$ monomers were performed at the B3LYP/6-311+G** and MP2/6-311+G** levels. The bond lengths (bond angles or dihedral angles) of the optimized complex were used for the partial optimized monomers and remained unchanged in the optimized process. The corresponding results are listed in Table III.

The results obtained at B3LYP/6-311+G** are in agreement with those obtained at the MP2/6-311+G** level (see Table III). The changes in N—O bond length and bond angle ($\angle$HNO) lead to N—H vibrational frequency, a slight blue shift relative to the HNO monomer, which indicates that the structure reorganization contributes in part to blue shifts in the H bond. The effect of N—O bond length change on the N—H vibrational frequency blue shift is larger than that of bond angle ($\angle$HNO) change. For the S—H vibrational frequency blue shift, the effect of the bond angle change on the vibrational frequency blue shift is larger than the other two effects of bond length and dihedral angles. From the above analysis, the structure reorganization of the bond length and bond angle contributes in part to the N—H vibrational frequency blue shift and that of the bond angles contributes in part to the S—H vibrational frequency blue shift.

Conclusions

Ab initio molecular orbital and DFT in conjunction with different basis sets calculations were performed to study the N—H$\cdots$O and S—H$\cdots$O blue-

TABLE III

Characteristics of optimized, partial optimized monomers and HNO· · ·$HFSO_2$ complex at B3LYP/6-311+G and MP2/6-311+G** levels (*r*-bond length; *A*-bond angle; *D*-dihedral angle).**

	Optimized monomer	Partial optimized monomer	Complex
	B3LYP/6-311+G**		
r (O6—N7) (Å)	1.1997		1.2041
A (O6N7H8) (°)	108.9		108.2
v (H8—N7) (cm^{-1})	2866		2965
v_r (H8—N7) (cm^{-1})		2886	
v_A (H8—N7) (cm^{-1})		2869	
r (S1—O2) (Å)	1.4367		1.4434
r (S1—O3) (Å)	1.4367		1.4367
r (S1—F5) (Å)	1.6266		1.6271
A (O2S1H4) (°)	109.9		109.8
A (O3S1H4) (°)	109.9		110.7
A (F5S1H4) (°)	94.4		95.3
D (O2S1H4F5) (°)	109.9		109.6
D (O3S1H4F5) (°)	−109.9		−110.7
v (S1—H4) (cm^{-1})	2562		2596
v_r (S1—H4) (cm^{-1})		2563	
v_A (S1—H4) (cm^{-1})		2565	
v_D (S1—H4) (cm^{-1})		2562	
	MP2/6-311+G**		
r (O6—N7) (Å)	1.2213		1.2238
A (O6N7H8) (°)	107.9		107.3
v (H8—N7) (cm^{-1})	3037		3117
v_r (H8—N7) (cm^{-1})		3042	
v_A (H8—N7) (cm^{-1})		3038	
r (S1—O2) (Å)	1.4314		1.4361
r (S1—O3) (Å)	1.4314		1.431
r (S1—F5) (Å)	1.6124		1.6117
A (O2S1H4) (°)	109.6		109.9
A (O3S1H4) (°)	109.6		110.4
A (F5S1H4) (°)	94.4		94.8
D (O2S1H4F5) (°)	109.8		109.4
D (O3S1H4F5) (°)	−109.8		−110.3
v (S1—H4) (cm^{-1})	2697		2733
v_r (S1—H4) (cm^{-1})		2697	
v_A (S1—H4) (cm^{-1})		2698	
v_D (S1—H4) (cm^{-1})		2697	

* v_r, effect of bond length on the vibrational frequencies; v_A, effect of bond angle on the vibrational frequencies; v_D, effect of dihedral angle on the vibrational frequencies.

shifted H-bonds in the HNO· · ·$HFSO_2$ complex. The geometric structures, vibrational frequencies, and interaction energies were calculated by both standard and CP-corrected methods. The contractions of N—H and S—H bond lengths and blue shifts of N—H and S—H vibrational frequencies were confirmed by all calculations. NBO analysis was applied to investigate the origin of blue shift H-bonds. From the NBO analysis, the decreases in the σ^*(N—H) and σ^*(S—H) are due to the electron density redistribution effect and contribute to the blue shifts of N—H and S—H vibrational frequencies. The changes in N—O bond length and bond angle (∠HNO) lead to N—H vibrational frequency, a slight blue shift relative to the HNO monomer. The effect of the N—O bond length change on the

N—H vibrational frequency blue shift is larger than that of the bond angle (∠HNO) change. For the S—H vibrational frequency blue shift, the effect of the bond angle change on the vibrational frequency blue shift is larger than the other two effects of bond length and dihedral angles.

References

1. Scheiner, S. Hydrogen Bonding; Oxford University Press: New York, 1997.
2. Karpfen, A. Adv Chem Phys 2002, 123, 469.
3. Dannenberg, J. J. J Mol Struct 2002, 615, 219.
4. Hobza, P. Int J Quantum Chem 2002, 90, 1071.
5. Jeffery P. G. A. An Introduction to Hydrogen Bonding; Oxford University Press: New York, 1997.
6. Hobza, P.; Špirko, V. Phys Chem Chem Phys 2003, 5, 1290.
7. Mrázková, E.; Hobza, P. J Phys Chem A 2003, 107, 1032.
8. Karpfen, A.; Kryachko, E. S. J Phys Chem A 2003, 107, 9724.
9. Kryachko, E. S.; Zeegers-Huyskens, T. J Phys Chem A 2001, 105, 7118.
10. McDowell, S. A. C. J Chem Phys 2003, 119, 3711.
11. Scheiner, S.; Kar, T. J Phys Chem A 2002, 106, 1784.
12. Kryachko, E. S.; Zeegers-Huyskens, T. J Phys Chem A 2003, 107, 7546.
13. Harada, T.; Yoshida, H.; Ohno, K.; Matsuura, H. Chem Phys Lett 2002, 362, 453.
14. Gu, Y.; Kar, T.; Scheiner, S. J Am Chem Soc 1999, 121, 9411.
15. Fang, Y.; Fan, J. M.; Liu, L.; Li, X. S.; Guo, Q. X. Chem Lett 2002, 31, 116.
16. Yang, Y.; Zhang, W. J.; Pei, S. Z.; Shao, J.; Huang, W.; Gao, X. M. J Mol Struct (Theochem) 2005, 732, 33.
17. Masunov, A.; Dannenberg, J. J.; Contreras, R. H. J Phys Chem A 2001, 105, 4737.
18. Yang, Y.; Zhang, W. J.; Gao, X. M. Int J Quantum Chem 2006, 106, 1199.
19. Bunte, S. W.; Rice, B. M.; Chabalowski, C. F. J Phys Chem A 1997, 101, 9430.
20. Jensen, F.; Foote, C. S. J Am Chem Soc 1988, 110, 2386.
21. Dianna, L.; Paul, M. J Phys Chem 1992, 96, 2471.
22. Boys, S. F.; Bernardi, F. Mol Phys 1970, 100, 65.
23. Reed, A. E.; Curtiss, L. A.; Weinhold, F. Chem Rev 1988, 88, 899.
24. Frisch, M. J.; Trucks, G. W.; Schlegel, H. B.; Scuseria, G. E.; Robb, M. A.; Cheeseman, J. R.; Montgomery, J. A., Jr.; Vreven, T.; Kudin, K. N.; Burant, J. C.; Millam, J. M.; Iyengar, S. S.; Tomasi, J.; Barone, V.; Mennucci, B.; Cossi, M.; Scalmani, G.; Rega, N.; Petersson, G. A.; Nakatsuji, H.; Hada, M.; Ehara, M.; Toyota, K.; Fukuda, R.; Hasegawa, J.; Ishida, M.; Nakajima, T.; Honda, Y.; Kitao, O.; Nakai, H.; Klene, M.; Li, X.; Knox, J. E.; Hratchian, H. P.; Cross, J. B.; Adamo, C.; Jaramillo, J.; Gomperts, R.; Stratmann, R. E.; Yazyev, O.; Austin, A. J.; Cammi, R.; Pomelli, C.; Ochterski, J. W.; Ayala, P. Y.; Morokuma, K.; Voth, G. A.; Salvador, P.; Dannenberg, J. J.; Zakrzewski, V. G.; Dapprich, S.; Daniels, A. D.; Strain, M. C.; Farkas, O.; Malick, D. K.; Rabuck, A. D.; Raghavachari, K.; Foresman, J. B.; Ortiz, J. V.; Cui, Q.; Baboul, A. G.; Clifford, S.; Cioslowski, J.; Stefanov, B. B.; Liu, G.; Liashenko, A.; Piskorz, P.; Komaromi, I.; Martin, R. L.; Fox, D. J.; Keith, T.; Al-Laham, M. A.; Peng, C. Y.; Nanayakkara, A.; Challacombe, M.; Gill, P. M. W.; Johnson, B.; Chen, W.; Wong, M. W.; Gonzalez, C.; Pople, J. A. Gaussian: Pittsburgh, PA, 2003.
25. Hobza, P.; Havlas, Z. Theor Chem Acc 1998, 99, 372.
26. Chocholouşová, J.; Špirko, V.; Hobza, P. Phys Chem Chem Phys 2004, 6, 37.
27. Alabugin, I. V.; Manoharan, M.; Peabody, S.; Weinhold, F. J Am Chem Soc 2003, 125, 5973.